第34卷 第3期 焊 接 学 报 Vol. 34 No. 3
2013年3月 TRANSACTIONS OF THE CHINA WELDING INSTITUTION March 2013

随焊冲击碾压整形对低匹配等承载接头硬度与残余应力的影响

杨建国[1]， 王佳杰[2]， 董志波[2]， 方洪渊[2]， 周立鹏[3]
（1. 浙江工业大学 化工机械设计研究所，杭州 310014；2. 哈尔滨工业大学 先进焊接与连接国家重点实验室，哈尔滨 150001；3. 中广核检测技术有限公司 苏州分公司，苏州 215004）

摘 要： 随焊冲击碾压整形（weld shaping with trailing impact rolling，WSTIR）是一种能够降低应力变形、提高承载能力的随焊整形新方法．分别对原始焊态的低匹配等承载接头与随焊冲击碾压整形的低匹配等承载接头进行了硬度试验和残余应力试验．结果表明，随焊整形等承载接头焊缝表面、焊趾处表面的硬度显著高于原始焊态等承载接头的硬度，说明随焊冲击碾压整形对接头承载的关键区域有加工硬化的效果；随焊整形低匹配等承载接头各点的纵向和横向残余应力明显低于原始焊态等承载接头相应位置的纵向和横向残余应力，甚至在随焊整形接头的焊缝中心以及焊趾附近纵向均出现了残余压应力，残余压应力的引入必然能显著地提高低匹配接头承载能力．

关键词： 低匹配等承载接头； 随焊冲击碾压整形； 维氏硬度； 残余应力
中图分类号： TG404 **文献标识码：** A **文章编号：** 0253－360X（2013）03－0037－04

杨建国

0 序 言

低匹配接头可以使焊缝获得良好的塑韧性、降低冷裂倾向[1,2]，所以低匹配接头越来越受到重视．但是低匹配接头承载能力有所降低．通过机械打磨、焊趾 TIG 熔修、锤击、超声冲击、低相变点焊条熔修等工艺方法[3-5]，可以提高接头的承载能力．最近相关的研究表明[6,7]，低匹配接头通过部分余高参与承载、几何形状优化可以获得与母材具有相等承载能力的等承载接头．而获得低匹配承载接头常采用机械加工方法，但是机械加工增加了工作强度、降低了工作效率，不利于承受疲劳载荷，阻碍了等承载接头的推广和应用．随焊冲击碾压方法可降低焊缝残余应力变形、防止热裂纹[8]，而随焊冲击碾压整形方法则是一种新型的随焊整形工艺，具有轻便、可靠、高效、劳动强度低等特点，还可提高接头的静载强度和疲劳强度[9]，弥补了机械加工方法的不足．

文中针对随焊冲击碾压整形的低匹配等承载接头与原始焊态的低匹配等承载接头的硬度和残余应力进行了试验研究，探讨这种方法对提高低匹配接头承载能力的力学机制提供理论的基础与依据．

收稿日期：2012－11－05
基金项目：先进焊接与连接国家重点实验室开放课题研究基金资助

1 随焊冲击碾压整形方法

图 1 为随焊冲击碾压接头整形装置试验平台，主要由压缩空气储气瓶、空气锤、固定支座、冲击碾压整形装置及工作台组成．其工作过程：储气瓶存满压缩空气，调节气瓶阀门气流量，将空气锤调至轻微震动状态，此时将 TIG 电弧引燃，TIG 电弧加热焊缝而不使其熔化，调整工作台行走，再调整气瓶流量，随焊整形开始．此时将随焊整形装置的前碾压轮作用于塑性变形温度区间的焊缝及焊趾处金属

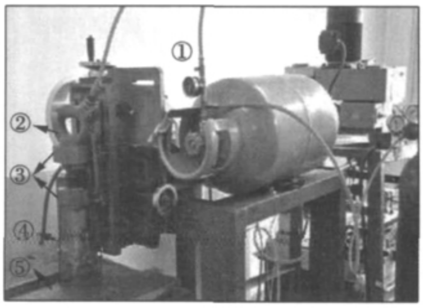

①. 压缩空气储气瓶 ②. 气锤 ③. 固定支座
④. 冲击碾压整形装置 ⑤. 工作台

图 1 随焊冲击碾压整形试验平台
Fig. 1 Test platform of WSTIR

上，通过冲击碾压初步整形获得需要的圆滑过渡焊趾形状及初步获得接头形状. 同时后碾压轮紧跟其后作用在仍具有一定温度的焊缝金属上，再次进行冲击碾压整形，以最终获得所需的余高高度、余高宽度和焊趾圆弧过渡半径等接头形状，达到随焊整形的效果. 当随焊整形完毕，关闭电弧及气阀.

图2为随焊冲击碾压整形装置. 前后碾压轮均由Gr15材料制成. 前后碾压轮焊趾半径分别为8，10 mm，前碾压轮深度大于后碾压轮深度，前后碾压轮成形宽度相等. 随焊冲击碾压装置具有结构简单、轻便、可靠、高效，还能够减小劳动强度，有利于等承载接头技术的推广和应用.

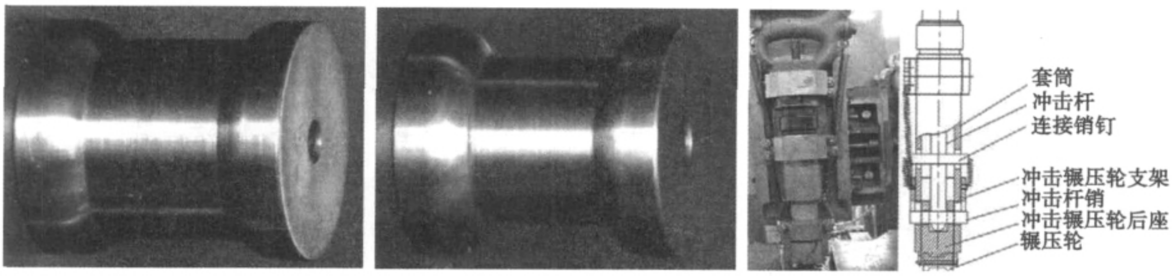

(a) 前碾压轮　(b) 后碾压轮　(c) 整体图

图2　随焊冲击碾压整形装置
Fig. 2　Device of WSTIR

2　试验材料及方法

试验母材为Q620-CF钢，厚度为8 mm，利用E4303焊条施焊而成，焊接材料性能参数见表1. X形坡口，坡口角度60°，钝边高2 mm，间隙2 mm. 先进行打底焊，然后进行坡口填充焊及盖面加宽焊，在焊前都要进行清根处理. 盖面加宽焊时要对称交错焊接，严格控制角变形. 焊接过程见图3. 打底焊接参数为：焊接电流130 A，电弧电压22 V，焊接速度200～250 mm/s；填充及盖面焊接参数为：焊接电流160 A，电弧电压26 V，焊接速度200～250 mm/s. 满足等承载要求的带有余高且表面平整的低匹配接头形状参数为：余高高度4 mm、焊盖面焊道半宽为18 mm、趾圆弧过渡半径8 mm. 利用随焊整形装置对上述低匹配等承载接头进行随焊整形. TIG电弧加热参数见表2.

表1　焊接材料性能参数
Table 1　Welding material properties parameters

焊接材料	屈服强度 $R_{eL0.2}$/MPa	抗拉强度 R_m/MPa	断后伸长率 A(%)
母材Q620-CF	629	890	19.2
焊缝J422	365	475	35.6

硬度试验采用HVS-5型维氏硬度计，压头载荷为3 N，作用时间10 s. 测量点位置如图4中接头轮廓线上黑色圆点所示，三个测量区域分别为焊缝表面A区、焊趾处表面B区和带有余高且表面平整的拐角处表面C区，测量点的间距为1 mm.

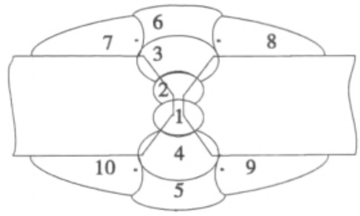

图3　焊接过程示意图
Fig. 3　Welding process schematic diagram

表2　TIG电弧加热参数
Table 2　TIG arc heating parameters

电源类型	钨极直径 D/mm	焊接电流 I/A	电弧电压 U/V	焊接速度 v/(mm·s^{-1})	保护气体
直流	3.2	100	20	0.5	氩气

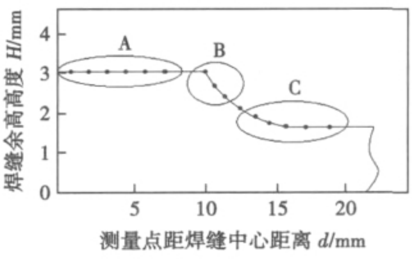

图4　硬度测量点位置
Fig. 4　Measuring point position of hardness

文中使用盲孔法分别对垂直焊缝长度方向以及焊趾处的纵向残余应力和横向残余应力进行测试. 设备为 CM-1J-20 型静态应变，测量点位置分别如图 5所示. 六个测量点垂直于焊缝长度方向. 第一个测试点距离起弧端的距离大约 50 mm，即图 5 中所示的 0 点，第二个测试点位于焊趾附近，距离焊缝中心 25 mm，其余测试点之间依次间隔为 10 mm. 焊趾处 a，b，c，d 四个测量点依次间隔为 10 mm.

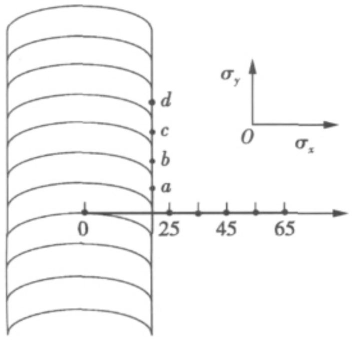

图 5　残余应力测量位置(mm)
Fig. 5　Measuring point position of residual stress

3　随焊整形对硬度的影响

两种接头硬度测量结果如图 6 所示. 结果表明，随焊整形等承载接头 A，B 区的硬度值显著高于原始焊态等承载接头相应区域的硬度值，A 区的硬度差别最大，B 区的硬度差别次之，C 区的硬度值差别最小. 说明随焊冲击碾压整形对焊缝表面和焊趾处表面金属的冲击碾压作用较大，而对平余高拐角处表面冲击碾压作用较小，恰恰焊缝和焊趾处为平余高对接接头承载能力大小的关键部位. 等承载接头随焊整形后硬度值提高，反映了随焊整形设备对等承载接头承载的关键区域有加工硬化的效果. 对于绝大部分金属材料而言，硬度是表征材料弹性、塑性、韧性和形变硬化等的一个综合物理量[10]. 一般来说，材料的硬度越高，则强度越高. 随焊整形后硬度提高也说明了文献 [9] 对静载与疲劳强度等力学性能的提高有着积极的贡献.

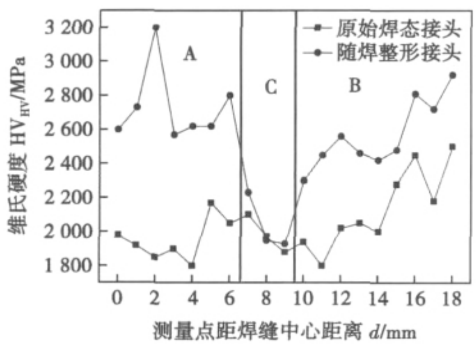

图 6　两种接头的硬度测量结果
Fig. 6　Hardness test result of two kinds of joints

4　随焊整形对残余应力的影响

两种接头纵向与横向残余应力的测量结果分别如图 7 和图 8 所示. 结果表明，与原始焊态等承载接头相比，随焊整形低匹配等承载接头的焊缝与焊趾附近各点纵向残余应力明显降低，而各点的横向残余应力均低于原始焊态等承载接头相应位置的横向残余应力. 对于原始焊态等承载接头而言，远离焊缝中心，纵向残余应力先降低再升高，且应力均为拉应力; 对于随焊整形低匹配等承载接头而言，焊缝中心以及焊趾附近纵向均出现压应力，远离焊趾处的纵向位置出现拉应力. 原始焊态接头焊缝中心处的纵向残余应力(357 MPa)几乎达到焊缝金属的屈服强度(365 MPa)，而随焊整形等承载接头焊缝中

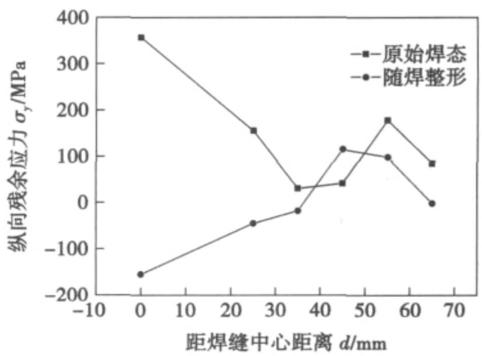

图 7　垂直于焊缝长度方向的纵向残余应力
Fig. 7　Longitudinal residual stress at vertical weld seams direction

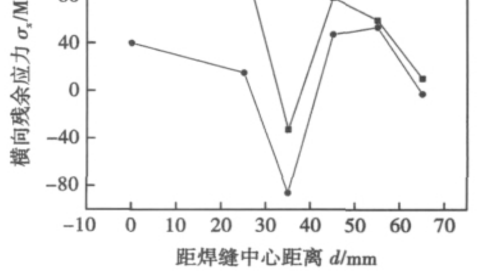

图 8　垂直于焊缝长度方向的横向残余应力
Fig. 8　Transverse residual stress at vertical weld seams direction

心纵向为残余压应力(-155 MPa). 原始焊态等承载接头焊趾附近点纵向应力为拉应力(155 MPa),而随焊整形等承载接头焊趾附近点纵向应力为压应力(-45 MPa). 这与随焊整形主要作用于焊缝中心以及焊趾附近金属位置有关. 因此,随焊冲击碾压整形设备的作用能够降低承载接头承载关键区域的残余应力,甚至引入残余压应力场,这必然显著地提高低匹配接头静载拉伸和疲劳承载能力[9].

焊趾处的纵向残余应力与横向残余应力的测量结果分别如图9和图10所示. 结果表明,随焊整形等承载接头焊趾附近的纵向残余应力和横向残余应力均显著低于原始焊态等承载接头相应位置的残余应力,纵向甚至出现残余压应力. 焊趾处残余应力的比较结果能进一步说明随焊整形能够降低接头残余拉应力,有利于提高接头的承载能力[9].

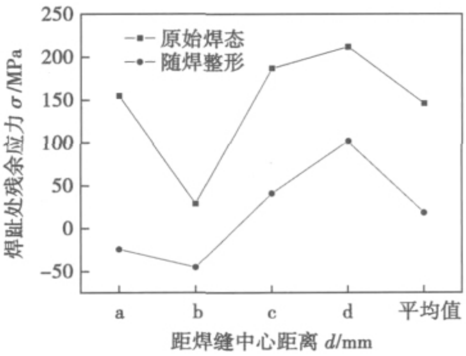

图9 焊趾处纵向残余应力
Fig. 9 Longitudinal residual stress at weld toe

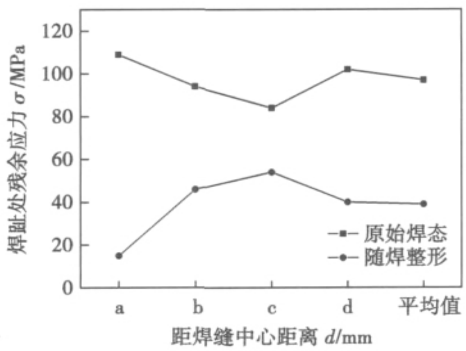

图10 焊趾处横向残余应力
Fig. 10 Transverse residual stress at weld toe

5 结 论

(1) 硬度试验结果表明,随焊整形等承载接头焊缝表面、焊趾处表面的硬度显著高于原始焊态等承载接头的硬度,焊缝表面区的硬度差别最大,焊趾处表面的硬度差别次之,平余高拐角处表面的硬度值差别最小,说明随焊冲击碾压整形对接头承载关键区域有加工硬化的效果.

(2) 残余应力试验结果表明,与原始焊态等承载接头相比,随焊整形低匹配等承载接头焊缝与焊趾附近各点纵向残余应力明显降低,而各点的横向残余应力均降低,甚至在随焊整形接头的焊缝中心以及焊趾附近纵向均出现了压应力. 残余压应力的引入有利于提高低匹配接头承载能力.

参考文献:

[1] Irving B U S. Navy maintains high interest in funding for welding research [J]. Welding Journal, 1995, 74(3): 41-47.

[2] Kim Y J, Schwalbe K H. Numerical analyses of strength mismatch effect on local stresses for ideally plastic materials [J]. Engineering Fracture Mechanics, 2004, 71: 1177-1199.

[3] Kirkhope K J, Bell R, Caron L. Weld detail fatigue life improvement techniques, part 1 review [J]. Marine Structures, 1999, 12: 447-474.

[4] Sonsino C M. Fatigue life improvement of welded structures by post-weld treatments and some limitations by geometry and loading mode [J]. Revue de Metallurgie, 2007, 104(1): 51-57.

[5] 王东坡, 周 达. 超声冲击法提高焊接接头疲劳强度的机理分析 [J]. 天津大学学报, 2007, 40(5): 623-628.
Wang Dongpo, Zhou Da. Mechanism analysis of fatigue strength improvement of welded joints by ultrasonic peening method [J]. Journal of Tianjin University, 2007, 40(5): 623-628.

[6] 赵智力, 方洪渊, 杨建国, 等. 一种针对低匹配焊接接头的"等承载"设计方法 [J]. 焊接学报, 2011, 32(4): 87-90.
Zhao Zhili, Fang Hongyuan, Yang Jianguo, *et al*. A design method ofequal load-carrying capacity for under-matching weld joints [J]. Transactions of the China Welding Institution, 2011, 32(4): 87-90.

[7] 王佳杰, 董志波, 刘雪松, 等. 弹性阶段低匹配对接接头三点弯曲余高形状设计 [J]. 焊接学报, 2012, 33(8): 37-40.
Wang Jiajie, Dong Zhibo, Liu Xuesong, *et al*. Shape design of the reinforcement for under-matched butt joints under the three-point bending load in elastic stage [J]. Transactions of the China Welding Institution, 2012, 33(8): 37-40.

[8] 范成磊, 方洪渊, 陶 军, 等. 随焊冲击碾压减小应力变形防止热裂纹应变场分析 [J]. 焊接学报, 2004, 25(6): 47-50.
Fan Chenglei, Fang Hongyuan, Tao Jun, *et al*. Strain field analysis of weld with trailing impact rolling to control residual stress and distortion and prevent hot cracking [J]. Transactions of the China Welding Institution, 2004, 25(6): 47-50.

[9] 王佳杰, 杨建国, 张敬强, 等. 随焊冲击碾压整形新方法及等承载接头拉伸与疲劳性能 [J]. 焊接学报, 2012, 33(10): 35-38.
Wang Jiajie, Yang Jianguo, Zhang Jingqiang, *et al*. A new weld shaping method with trailing impact rolling and tensile and fatigue properties for equal load-carrying capacity joint [J]. Transactions of the China Welding Institution, 2012, 33(10): 35-38.

[10] 杨道明, 朱 勋, 李紫桐. 金属力学性能与失效分析 [M]. 北京: 冶金工业出版, 1991.

作者简介: 杨建国,男,1975年出生,博士,副教授,硕士研究生导师. 主要从事焊接结构力学与可靠性方面的科研和教学工作. 发表论文100余篇. Email: yangjg@zjut.edu.cn

joint was excellent due to the slight interface migration, and fracture occurred in the top sheet. However, when the interfaces at both sides of weld moved downward, fracture occurred in the bottom sheet. The shear strength decreased with increase of the height of interface migration. The shear strength was higher when the load was exerted on the advancing side than on the retreating side.

Key words: friction stir welding; lap joint; plunge depth of shoulder; interface migration; mechanical properties

Effects of welding parameters on temperature field in GTAW ZHAO Ming, DU Dandan, LUO Detong (College of Mechanical and Electronic Engineering, China University of Petroleum, Qingdao 266580, China). pp 20 – 24

Abstract: Numerical analysis of heat transfer in gas tungsten arc welding (GTAW) process was conducted with ANSYS software. The calculated results of transient evolution of isotherms during continuous welding for 20 s and cooling for 20 s show that the workpiece was completely penetrated at 5 s after the arc was struck, however, the molten pool totally disappeared within 1 s after the arc moved away. During the welding process, the high-temperature region moved simultaneously with the arc. When the arc moved away, the cooling stage began, the zone with high temperature gradually moved backward (relative to the welding direction) and cooled to ambient temperature. The predicted thermal cycles at different points with the same intervals on top surface along the welding direction displayed that the temperature rising curves have the same trend in quasi-steady state, while clear differences existed between the temperature decreasing curves because the latent heat was released when the molten metal solidified. The temperature decreased faster at points closer to the weld crater. The influences of welding current, welding speed and concentration parameter on the heat transfer were analyzed, and then these parameters were optimized.

Key words: Gaussian heat source; distribution parameter of heat flux; gas tungsten arc welding; numerical analysis

Microstructure and mechanical properties in heat-affected zone of large-thickness steel ingot cut with oxygen-propane flame HAN Yongkui[1], WANG Zhixin[1], YAN Jiashu[1], LIN Yaowu[2], ZHAO Xianhong[2], MEI Longtian[2] (1. Harbin Welding Institute, China Academy of Machinery Science and Technology, Harbin 150080, China; 2. HengDing Shipbuilding Heavy Industry Co., Ltd., Suzhou 215513, China). pp 25 – 28, 32

Abstract: The machining allowance of precision metal cutting machine tools depends on the microstructure evolution in heat-affected zone during flame cutting. In this paper, 900 mm thick 34CrNiMo6 steel and 450 mm thick 45 carbon steel ingots were cut using an oxygen-propane flame. Then, the macroscopic morphology and microstructure in the heat-affected zone were examined to analyze the influence of microstructure evolution on the performance of workpieces. The range of heat-affected zone and machining allowance were determined to optimize the parameters during cutting and after cutting process.

Key words: flame cutting; large cross-section; steel; microstructure; heat-affected zone

Fatigue crack propagation of aluminum alloy based on acoustic emission monitoring ZHU Ronghua, GANG Tie (State Key Laboratory of Advanced Welding and Joining, Harbin Institute of Technology, Harbin 150001, China). pp 29 – 32

Abstract: The acoustic emission technique was used to monitor the fatigue crack propagation of 7N01 aluminum alloy single-edge notched three-point bend specimens under different stress ratio and peak load. The relationship between the crack growth rate, acoustic emission count rate and stress intensity factor range was established. The results show that most of the acoustic emission signals were produced in the low stress cyclic loading stage because the acoustic emission activity in low-stress phase was mainly related to the plastic deformation and crack closure in crack tip, and the acoustic emission count exponentially grew with the stress intensity factor. Based on the relationship between the acoustic emission count rate and crack growth rate, the remaining life of fatigue-damaged structures could be predicted.

Key words: aluminum alloy; acoustic emission; fatigue; counts

Arc pressure measurement and analysis of coupling arc AA-TIG HUANG Yong[1,2], QU Huaiyu[1], FAN Ding[1,2], LIU Ruilin[1], KANG Zaixiang[1], WANG Xinxin[1] (1. State Key Laboratory of Gansu Advanced Non-ferrous Metal Materials, Lanzhou University of Technology, Lanzhou 730050, China; 2. Key Laboratory of Non-ferrous Metal Alloys, The Ministry of Education, Lanzhou University of Technology, Lanzhou 730050, China). pp 33 – 36

Abstract: In order to study the coupling arc AA-TIG (arc assisted activating tungsten inert gas) welding, a static keyhole method was used to measure the arc pressure with stainless steel as the anode. The influence of main process parameters on the distribution of arc pressure was analyzed. Compared to the conventional TIG welding process under the same conditions, the peak value of arc pressure during the coupling arc AA-TIG welding was significantly reduced. With the welding current decreasing, the electrode distance increasing, the arc length increasing and the oxygen content of the assisted arc decreasing, the peak value of arc pressure in coupling AA-TIG welding decreased. The distribution of arc pressure was in concordance with Gaussian distribution at 2 mm electrode distance. With the electrode distance increasing, the distribution gradually turned into bimodal distribution.

Key words: AA-TIG; coupling arc; oxygen element; arc pressure; high-speed welding

Influence of weld shaping with trailing impact rolling on hardness and residual stress of under-matched equal load-carrying joint YANG Jianguo[1], WANG Jiajie[2], DONG Zhibo[2], FANG Hong yuan[2], ZHOU Lipeng[3] (1. Institute of Process Equipment and Control Engineering, Zhejiang University of Technology, Hangzhou 310014, China; 2. State Key Laboratory of Advanced Welding and Joining, Harbin Institute of Technology, Harbin 150001, China; 3. CGNPC Inspection Technology Co. Ltd, Suzhou 215004, China). pp 37 – 40

Abstract: Weld shaping with trailing impact rolling (WSTIR) is a new weld shaping and modifying technique to reduce the residual stress and distortion and improve load-carrying capacity of under-matched joint. Vickers hardness test and residual stress test were carried out for under-matched equal load-carrying joint in as-welded state and after WSTIR, respectively. Hardness test results show that the surface hardness, both on weld beam and weld toe, for equal load-carrying joint after WSTIR was significantly higher than that in as-welded state, which revealed that WSTIR had work-hardening effect on key load-carrying areas for equal load-carrying joint. Residual stress test results show that both longitudinal and transverse residual stresses on under-matched joint after WSTIR were remarkably lower than those in as-welded state. Especially, longitudinal compressive residual stress appeared in the weld beam and weld toe after WSTIR, which can undoubtedly improve the load-carrying capacity for under-matched joint.

Key words: under-matched equal load-carrying joint; weld shaping with trailing impact rolling; Vickers hardness; residual stress

Microstructure and properties of vacuum brazed joint between super-Ni/NiCr laminated composite and Cr18-Ni8 steel WU Na, LI Yajiang, WANG Juan (Key Laboratory for Liquid-Solid Structural Evolution and Processing of Materials (Ministry of Education), Shandong University, Jinan 250061, China). pp 41 – 44

Abstract: Vacuum brazing of super-Ni/NiCr laminated composite to Cr18-Ni8 steel was performed using Ni-Cr-Si-B amorphous foil. Microstructure characteristic and shear strength of the brazed joints were investigated by scanning electron microscopy (SEM), energy-dispersive spectroscopy (EDS), microsclerometer and mechanical universal testing machine. The experimental results showed that the Ni-Cr-Si-B amorphous foil exhibited good wettability on super-Ni/NiCr laminated composite. The brazed region consisted of γ-Ni solid solution and Ni3B. Dissolution and diffusion occurred between the filler metal and super-Ni/NiCr laminated composite. An excellent bonding was obtained between them. An interface consisting of fine boride particles formed between the filler metal and Cr18-Ni8 stainless steel. The shear strength of the brazed joint reached 170MPa, and the fracture morphology displayed stepped fracture surface with some dimples and tearing feature in the brazed region.

Key words: laminated composite materials; vacuum brazing; microstructure; the shear strength

Recognition of weld defects based on multi-probe source data fusion HU Wengang, GANG Tie (State Key Laboratory of Advanced Welding and Joining, Harbin Institute of Technology, Harbin 150001, China). pp 45 – 48

Abstract: The recognition of defections is still a difficulty in non-destructive testing field. A new method for recognition of weld defects based on multi-probe source data fusion was proposed in this paper, which improved the reliability of detection and accuracy of defection recognition. Several welds, containing defects of hole, slag and crack, lack of penetration and lack of fusion were respectively inspected by two probes which possessed different angles of incidence. Then the ultrasonic signal features of defect echo were extracted. Finally, an intellectualized pattern classifier with two-level feature fusion and decision fusion was developed to realize the defect recognition with data fusion. BP neural network was selected as the classifier of feature fusion to obtain the basic probability function of each probe and probability value of each type of defect. Then D-S evidential theory was used to combine the probability function of each probe and to carry out the defect recognition. The results show that the multi-probe information could be effectively fused, and the recognition rate of weld defect was improved.

Key words: ultrasonic testing; defect recognition; data fusion; neural network; D-S evidential theory

Influence of welding time on performance and failure mode of hot stamping boron high strength steel spot-welded joints
CHEN Shujun, HAO Sufeng, YU Yang, BAI Lilai (Advanced Manufacturing Technology for Automotive Structural Components Engineering Center of the Education Ministry, Beijing University of Technology, Beijing 100124, China). pp 49 – 52, 92

Abstract: The characteristics of large resistivity, high peak temperature in welding thermal cycle, fast rising rate of temperature and uneven local cooling rate determined the heterogeneity in resistance spot-welded joints of hot stamping boron high strength steel, which resulted in three different failure modes of the joints. The effects of welding time on microhardness, bearing performance, failure modes of the resultant joints were studied, and the failure mechanism was investigated. The results show that the capacities of bearing and energy absorption between 400 ms and 600 ms of welding time were equivalent, and the nugget pull-out could not be the standard for evaluating the quality of joints. The welding defects, stress concentration and local toughness deterioration in HAZ were three main factors that affected the failure of the joints.

Key words: hot stamping boron high strength steel; failure mode; interface failure; nugget pullout

Effect of wire-wire distance on arc stability during laser-twin-arc hybrid welding process GU Xiaoyan[1], LI Huan[1], YANG Lijun[1], GAO Ying[2] (1. Tianjin Key Laboratory of Advanced Joining Technology, Tianjin University, Tianjin 300072, China; 2. Tianjin Key Laboratory of High-Speed Cutting and Precision Machining, Tianjin University of Technology and Education, Tianjin 300222, China). pp 53 – 56, 60

Abstract: Multi-information fusion including current, voltage and high-speed camera signals was used to investigate the effect of wire-wire distance on the arc behavior, droplet transfer and weld formation. The largest Lyapunov exponents of welding current during laser-twin-arc hybrid welding process were numerically evaluated in different wire-wire distances based on chaos theory. The results clearly demonstrate that the laser-twin-arc welding process was in chaotic state. Arc shape and droplet transfer were affected by the interactions of laser-induced plasma and arc plasma in laser-twin-arc hybrid welding process, which